CORE
Metadata, citation and similar papers at core.ac.uk
Provided by RERO DOC Digital Library

Catalysis Letters Vol. 104, Nos. 1–2, October 2005 (© 2005)
DOI: 10.1007/s10562-005-7429-y

Flame-made alumina supported Pd–Pt nanoparticles: structural properties and catalytic behavior in methane combustion

Reto Strobel[a,b], Jan-Dierk Grunwaldt[b], Adrian Camenzind[a], Sotiris E. Pratsinis[a], and Alfons Baiker[b,*]

[a]*Particle Technology Laboratory, Department of Mechanical and Process Engineering, ETH Zentrum, Swiss Federal Institute of Technology, CH-8092 Zurich, Switzerland*

[b]*Department of Chemistry and Applied Biosciences, ETH Hönggerberg, Swiss Federal Institute of Technology, CH-8093 Zurich, Switzerland*

Received 10 May 2005; accepted 1 July 2005

Bimetallic palladium–platinum nanoparticles supported on alumina were prepared by flame spray pyrolysis. The as-prepared materials were characterized by scanning transmission electron microscopy (STEM), CO chemisorption, nitrogen adsorption (BET), X-ray diffraction (XRD), temperature programmed reduction (TPR), thermogravimetric analysis (TGA) and extended X-ray absorption fine structure (EXAFS) spectroscopy. The materials were tested for the catalytic combustion of methane with a focus on the thermal stability of the noble metal particles. After flame synthesis the noble metal components of the materials were predominantly in oxidized state and finely dispersed on the alumina matrix. Reduction afforded small bimetallic Pd–Pt alloy particles (<5 nm) supported on Al_2O_3 ceramic nanoparticles. The addition of small amounts of platinum made the palladium particles more resistant against sintering at high temperatures and further lowered the deactivation observed during methane combustion.

KEY WORDS: flame spray pyrolysis; thermal stability; bimetallic catalysts; catalytic combustion; Pd–Pt nanoparticles; EXAFS.

1. Introduction

Catalytic combustion of methane, the main component in natural gas, has been extensively studied during the past years and progress has been covered in several recent review articles [1–3]. Natural gas is a relatively clean source of energy, since the combustion of methane produces the highest amount of energy per CO_2 molecule. The use of a catalyst reduces the emission of carbon monoxide, soot and unburned hydrocarbons and, due to lower process temperatures compared to traditional homogeneous combustion, prevents the formation of thermal NO_x. The catalytic process further improves the process stability and makes it possible to obtain complete oxidation of the fuel at low temperatures with low fuel-to-air ratios.

Palladium is an often used catalyst with high activity in methane combustion. However, the use of palladium has some drawbacks, including large hysteresis effects due to the transformation of palladium oxide into metallic palladium and deactivation at higher temperatures due to sintering. In order to stabilize the catalyst, the addition of another noble metal such as Pt, Rh, Ru, etc. has been proposed by several authors. Ersson *et al.* [4] studied the influence of Pt and Rh on the behavior of Pd/Al_2O_3 catalysts and found an increased stability when Pt was used as a co-metal. Narui *et al.* [5] observed decreased sintering of the metal particles when platinum was added to palladium. The preparation method can have significant influence on the activity and stability of bimetallic Pd–Pt catalysts [6,7]. In general, bimetallic catalysts are prepared either by nonselective or selective deposition of the metals on the supporting material [8]. Only the selective deposition by redox methods [9], surface organometallic chemistry [10] or the deposition of heterobinuclear complexes [11] assures the close vicinity of the two components leading to supported alloy particles. Alloy formation has been investigated in several studies and often evidenced using EXAFS [12–16].

Flame synthesis is a one-step preparation method for mixed oxides and supported noble metal catalysts [17]. Compared to conventional vapor-fed flame aerosol synthesis, as used for synthesis of Pt/TiO_2 [18], flame spray pyrolysis offers the possibility to use nonvolatile precursors and was applied for synthesis of Pt/Al_2O_3 and Pd/Al_2O_3 hydrogenation catalysts [19,20] as well as for Au supported on TiO_2 and SiO_2 [21]. Flame synthesis is used on large scale today to produce carbon black, fumed silica and titania pigments. In general, flame synthesis and especially flame spray pyrolysis are continuous, well controllable and versatile processes for the production of a wide variety of nanoparticles [22].

As shown earlier, flame made $Pd/La_2O_3/Al_2O_3$ catalysts show good performance in the combustion of methane and exhibit excellent thermal stability concerning the loss of specific surface area [23]. In this study flame spray pyrolysis was used as a single-step process for the synthesis of bimetallic Pt–Pd catalysts supported on alumina.

* To whom all correspondence should be addressed.
E-mail: baiker@chem.ethz.ch

1011-372X/05/1000–0009/0 © 2005 Springer Science+Business Media, Inc.

2. Experimental

2.1. Catalyst preparation

The experimental setup for the synthesis of Pd–Pt/Al_2O_3 catalysts by flame spray pyrolysis has been described earlier [24]. The precursor solution consisted of aluminium(III) sec-butoxide, palladium(II) acetylacetonate and platinum(II) acetylacetonate dissolved in a mixture of xylene and acetonitrile (2:1 vol%). The aluminium concentration was kept constant at 0.67 M for all experiments. The liquid precursor mixture was fed at 5 ml/min in the center of a methane/oxygen flame by a syringe pump (Inotech) and dispersed by oxygen (5 l/min), forming a fine spray. The pressure drop at the capillary tip was kept constant at 1.5 bar by adjusting the orifice gap area at the nozzle. The spray flame was surrounded and ignited by a small flame ring issuing from an annular gap (0.15 mm spacing, at a radius of 6 mm). The total gas flow rate through this premixed methane/oxygen supporting flame ring was 3.5 l/min with a CH_4/2 O_2 ratio of 0.92. Product particles were collected on a glass fiber filter (Whatmann GF/D, 25.7 cm in diameter) with the aid of a vacuum pump (Busch, Seco SV 1040C). The resulting material was designated as *w*Pd*x*Pt, where *w* and *x* denote the weight fraction in percent of Pd and Pt, respectively, and the balance was Al_2O_3. For all samples the total noble metal content was kept constant at 2.5 wt%. The mass fraction of platinum (W) in relation to the total mass of noble metals was defined as $W = m_{Pt}/(m_{Pt} + m_{Pd}) \cdot 100\%$.

2.2. Catalyst characterization

The specific surface area (SSA) of the as-prepared powders was determined by nitrogen adsorption at 77 K using the BET method (Micromeritics Tristar). The powder X-ray diffraction patterns were recorded with a Bruker D8 advance diffractometer.

For scanning transmission electron microscopy (STEM), the material was dispersed in ethanol and deposited onto a perforated carbon foil supported on a copper grid. The investigations were performed on a Tecnai F30 microscope (FEI (Eindhoven); field emission cathode, operated at 300 kV). Scanning transmission electron microscopy (STEM) images, obtained with a high-angle annular dark field (HAADF) detector, reveal the metal particles with bright contrast (Z contrast). The focused electron beam was then set on some of the bright points to analyze the ratio Pd:Pt of these particles qualitatively by energy dispersive X-ray spectroscopy (EDXS; detector (EDAX) attached to the Tecnai F30 microscope).

Extended X-ray absorption fine structure (EXAFS) spectroscopy measurements were carried out at beamline X1 at the Hamburger Synchrotronlabor (HASYLAB at DESY, Germany). A Si (311) double crystal was used for monochromatization of the beam. By detuning the crystals to 70% of the maximum intensity, higher harmonics were effectively eliminated. The measurements were carried out in a continuous-flow reactor cell, which allowed simultaneous gas analysis and structural studies [25,26]. The as-prepared powders were mounted in a capillary as described earlier [25] and reduced *in situ* by flowing 5% H_2/He at 250 °C prior to the measurements. Three ionization chambers were used to measure the incident and outcoming X-ray intensities, located before and after the *in situ* cell as well as after a Pd foil for energy calibration. The ionization chamber gases (Ar, Kr) and their pressure were adjusted in a way that about 10% were adsorbed in the first ionization chamber and 40% in the second and third ionization chamber. EXAFS spectra were taken around the Pd K-edge in the step-scanning mode between 24,000 and 25,800 eV. During dynamic changes (temperature, gas change) faster spectra in the region 24,300–24,600 eV were taken in the continuous scanning mode (QEXAFS). The EXAFS function was extracted using the WINXAS 3.0 software [27]. The EXAFS data were fitted in R-space. Scattering amplitudes and phase shifts of the Pd–Pd and the Pd–Pt shell (only first shell) were calculated using the FEFF6.0 code [28].

Noble metal dispersion was determined by CO-pulse chemisorption at 40 °C using a He flow of 50 ml/min and pulses of 0.5 ml (10% CO in He) on a Micromeritics Autochem II 2920 unit. Prior to the measurement, all samples were freshly reduced for 1 h at 250 °C under flowing hydrogen (20 ml/min) and then flushed by He (20 ml/min) at 260 °C for 90 min.

The oxidation behavior of palladium was measured by thermogravimetric analysis (TGA/SDTA851e, LF/1100 °C, Mettler Toledo AG). The powders were heated in nitrogen to 250 °C at 10 °C/min and held at this temperature for 30 min. Then the atmosphere was changed to air and two heating–cooling cycles from 250 °C to 1050 °C were recorded with a heating or cooling rate of ±20 °C/min.

Temperature programmed reduction of PdO by hydrogen was measured on a Micromeritics Autochem II 2920, equipped with a TCD-detector, by flowing a mixture of 5% H_2 in argon (20 ml/min). The temperature was ramped from −80 to 900 °C with the aid of a liquid nitrogen fed sub-ambient cooler at a heating rate of 10 °C/min. Prior to analysis, palladium was oxidized in flowing oxygen at 500 °C.

Methane oxidation was measured in a conventional fixed-bed flow microreactor at atmospheric pressure. The reactor, consisting of a quartz tube of 5 mm ID, was placed in an electric furnace. A mixture of 5 mg catalyst (100–250 μm) and 200 mg quartz sand (100–300 μm) was placed in the reactor and fixed with quartz wool. A thermocouple was inserted in the center of the catalyst bed. A mixture containing 1.0 vol% methane and 4.0 vol% oxygen in helium was flown through the reactor at 100 ml/min. Mass spectrometry (Thermostar,

Pfeiffer Vacuum) was used to determine all gas concentrations in the effluent gas stream. The transient behavior and conditioning/deactivation of the catalysts was measured by cycling the temperature several times from 200 °C up to 1000 °C at a heating or cooling rate of ±10 °C/min.

3. Results and discussion

3.1. Catalyst characterization

Bimetallic Pd–Pt catalysts supported on Al_2O_3 were prepared by single-step flame spray pyrolysis. The specific surface area of all as-prepared powders was around 120 m^2/g and not influenced by the noble metal composition. Figure 1a shows an STEM image of an as-prepared material, containing 1.5 wt% palladium and 1 wt% platinum. The noble metals form small particles in the range of 1–5 nm on top of agglomerated alumina nanoparticles. EDXS analysis ($d=2$ nm) of single noble metal particles revealed the coexistence of palladium and platinum in the same particle. After artificial sintering at 1000 °C, the noble metals formed large particles (figure 1b) in the range of the noble metal particle size observed after catalytic combustion [23]. The inset depicts a corresponding EDXS analysis of a single metal particle, showing the presence of Pt and Pd in the same particle after sintering at 1000 °C.

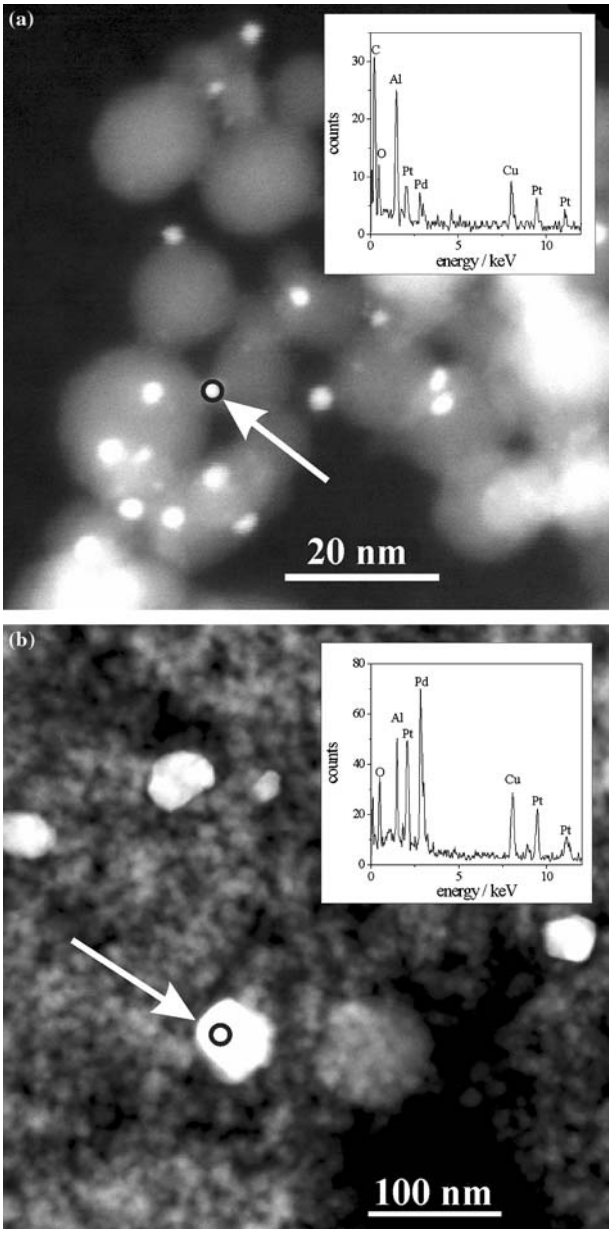

Figure 1. STEM images of as-prepared 1.5Pd1Pt (a) and after annealing at 1000 °C (b) with corresponding EDX analysis of an individual Pd–Pt particle.

Further evidence for alloy formation of the Pd–Pt particles emerged from EXAFS investigations. The radial distribution functions of the Fourier transformed EXAFS data (figure 2) show that the palladium is in oxidized state after preparation. No contribution at 2.8–3.5 Å is found, which would be characteristic for larger PdO particles (for reference spectra of PdO see for example [29]) or the possible formation of larger, oxidized Pt–Pd particles. Hence, palladium is finely dispersed in the oxide matrix. The EXAFS spectra also did not indicate any metallic palladium in the as-prepared samples. After reduction of the 1.5Pd1Pt catalyst with hydrogen, the backscattering of the nearest neighbors of the 1.5Pd1Pt sample differs from the pure 2.5Pd sample, indicating alloying of the Pt–Pd particles. This is supported also by fitting of the EXAFS data of the different samples (table 1, figure 3). Obviously, the Pd–Pt-based particles are alloyed after the reduction procedure. The number of Pt neighbors around the Pd absorber atoms decreases if the concentration of Pt decreases. In addition, both the low coordination number and the absence of higher shells in the EXAFS spectra indicate a small particle size. The number of nearest neighbors in the first coordination shell is significantly below 12 for both Pd and Pt–Pd samples. The absence of distinct reflections due to Pd or Pt in the XRD pattern of the as-prepared catalysts (not shown) and the STEM investigations (figure 1) give further evidence for the formation of small metal particles. In conclusion, the alloyed Pt–Pd-particles are not formed upon preparation but rather during the reduction in hydrogen. The good dispersion of both Pt and Pd in the matrix probably favours the formation of mixed Pt–Pd particles and not monometallic particles, as also observed when using other preparation methods [15,30,31].

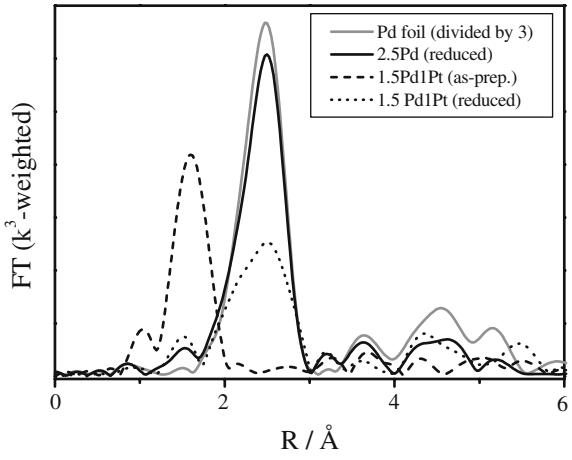

Figure 2. Comparison of Fourier transformed EXAFS data of the 1.5Pd1Pt catalyst before and after reduction in 5%H_2/He at 250 °C with the 2.5Pd catalyst and Pd foil.

The influence of platinum on the thermal stability of palladium, and vice versa, was investigated by sintering the as-prepared materials at 800 and 1000 °C for 4 h in air. Figure 4 depicts the relative amount of CO chemisorbed on the noble metals after this annealing as a function of the Pt mass fraction (W). After annealing at 800 °C pure platinum sintered strongly, whereas for the only palladium containing sample a lower sintering effect was observed. The addition of very small amounts of Pt to Pd ($W = 4\%$) stabilized the Pd particles and

Table 1
Structural parameters determined by fitting of EXAFS spectra at the Pd K-edge of selected Pd–Pt/Al_2O_3 catalysts after their in situ reduction in 5%H_2/He

Catalyst	A[a]–Bs[b]	r[c]/Å	N[d]	σ^{2}[e]/Å	ΔE_0[f]/eV	Residual[g]
1.5Pd1Pt	Pd–Pd	2.75	4.2	0.008	−3.5	3.1
	Pd–Pt	2.75	6.0	0.015[h]	0.35	
2Pd0.5Pt	Pd–Pd	2.75	7.0	0.007	−1.8	2.9
	Pd–Pt	2.75	4.0	0.017[h]	−2.07	
2.5Pd	Pd–Pd	2.75	8.6	0.007	−2.5	2.3
	Pd–Pt	–	–	–	–	
1.5Pd1Pt	Pd–Pd	2.75	5.0	0.0075[i]	−4.13	4.3
	Pd–Pt	2.75	3.6	0.0075[i]	−0.37	
2Pd0.5P	Pd–Pd	2.75	7.0	0.007[i]	−1.27	2.8
	Pd–Pt	2.75	1.5	0.007[i]	−0.45	

[a]Absorber.
[b]Backscatterer.
[c]Distance.
[d]Coordination number.
[e]Debye–Waller factor.
[f]Shift of the energy threshold.
[g]Quality of fit [27].
[h]Note the high Debye–Waller factor if that of the Pd–Pt and Pd–Pd shell are not corrected.
[i]Fixing the Debye–Waller factor of the Pd–Pt and the Pd–Pd shell to the same value.

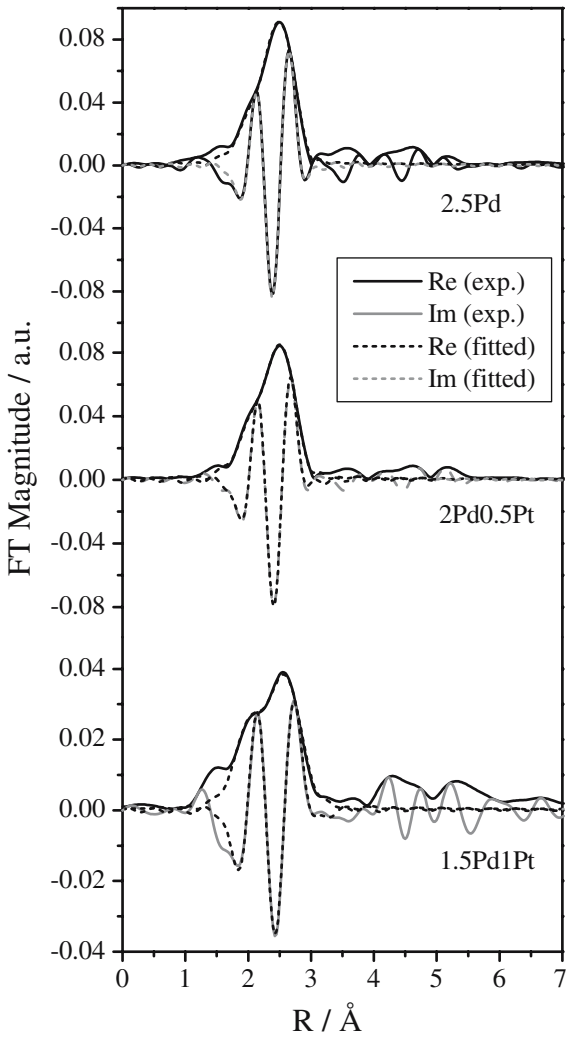

Figure 3. Experimental and fitted Fourier transformed k^3-weighted $\chi(k)$-functions of selected flame-made Pd- and Pd–Pt-based catalysts.

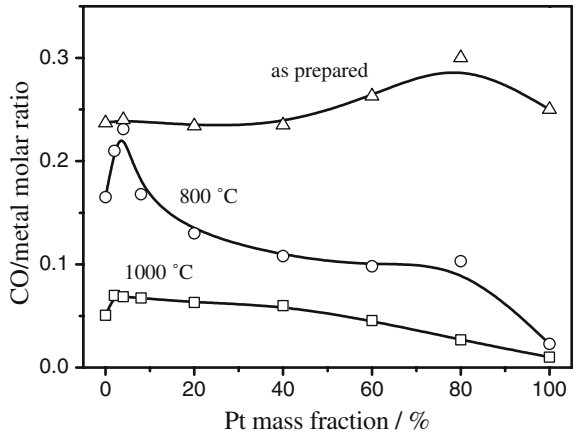

Figure 4. Molar ratio of CO chemisorbed to noble metal content of as-prepared bimetallic flame-made Pd–Pt catalysts and after annealing them at 800 °C and 1000 °C (air, 4 h).

prevented any sintering at 800 °C. Furthermore, Pd stabilized the Pt particles compared to pure Pt/Al_2O_3. At 1000 °C the noble metals sintered strongly, as shown by a drop in the amount of CO chemisorbed. Corresponding to the results at 800 °C even very small amounts of platinum stabilized the palladium particles, resulting in the smallest metal particles for Pt metal mass fractions between 2 and 14%.

X-ray diffraction patterns (figure 5) measured after annealing of the materials at 1000 °C showed the formation of crystalline M^0 and MO domains (M = Pd or Pt). A higher Pt mass fraction (W) increased the amount of crystalline M^0 and lowered the amount of MO.

Figure 6 depicts TPR profiles of the calcined materials (1000 °C) with the corresponding amounts of consumed and released hydrogen given in Table 2. The H_2:Pd ratio of the total amount of consumed hydrogen was similar for all samples (1–1.05) and close to the theoretical value of 1. In all samples palladium was reduced between 0 and 50 °C. The addition of platinum broadened the peaks and shifted the peak maximum to slightly lower temperatures. The release of hydrogen from bulk Pd–H species was observed at around 70 °C,

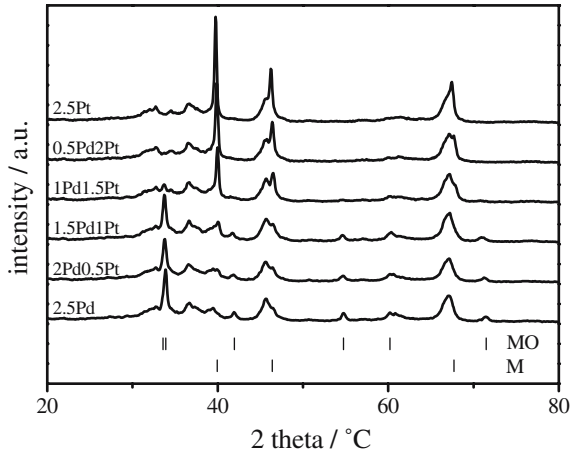

Figure 5. XRD pattern of $Pd–Pt/Al_2O_3$ after annealing at 1000 °C for 4 h. Peak positions of M^0 (Pd or Pt cubic) and MO (PdO or PtO tetragonal) are given at the bottom.

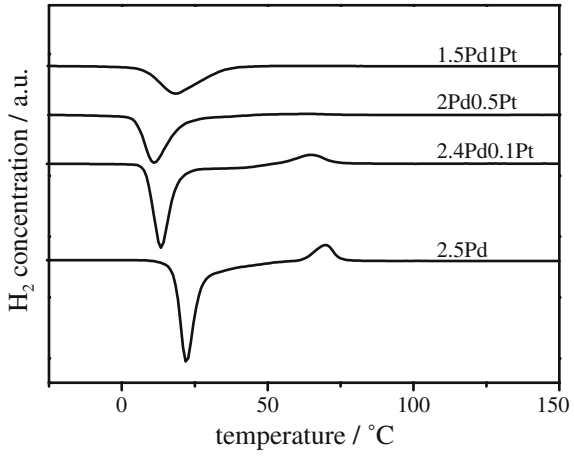

Figure 6. Temperature programmed reduction (TPR) profiles of bimetallic $Pd–Pt/Al_2O_3$ after sintering at 1000 °C.

Table 2
Temperatures of maximum hydrogen consumption (peak position) and amount of H_2 consumed and released during TPR of flame made Pd–Pt/Al_2O_3 after annealing at 1000 °C

Sample	1st peak pos. (°C)	2nd peak pos. (°C)	H_2 :Pd ads.[a]	H_2 :Pd rel.[b]	H_2 :Pd total[c]
2.5Pd	22	69	1.22	0.21	1.01
2Pd0.5Pt	13	65	1.18	0.18	1.00
1.5Pd1Pt	11	–	1.03	–	1.03
1Pd1.5Pt	18	–	1.05	–	1.05

[a] H_2/Pd ratio of consumed hydrogen during reduction (first peak).
[b] H_2/Pd ratio of released hydrogen from Pd–H (second peak).
[c] H_2/Pd ratio of the total amount of H_2 consumed (consumed–released hydrogen).

resulting in an increase of the hydrogen concentration. However, no hydrogen release occurred for Pt mass fractions higher than 4% (2.4Pd0.1Pt). The distortion by the added platinum atoms may lead to smaller palladium domains that are not capable to form bulk palladium hydride species [32]. The broadening of the hydrogen uptake peaks is an additional indication for this behavior as smaller Pd particles tend to show broader signals [23].

Figure 7 shows TGA profiles measured in air during the second heating/cooling cycle of as-prepared flame-made Pd–Pt catalysts. Upon heating of pure palladium supported on alumina (2.5Pd), PdO decomposed into Pd^0 between 850 and 950 °C and re-oxidized between 540 and 610 °C during cooling, as indicated by a decrease and increase in weight, respectively. The addition of small amounts of platinum resulted in two distinct steps for the reduction of PdO, one in the temperature range of the pure palladium and an additional one at lower temperatures (770–810 °C), which increased when more Pt was added. For Pt mass fractions higher than 20% only one reduction step was observed at lower temperatures. This behavior was also reported by others [4] and can be attributed to the promotion of PdO reduction by platinum addition.

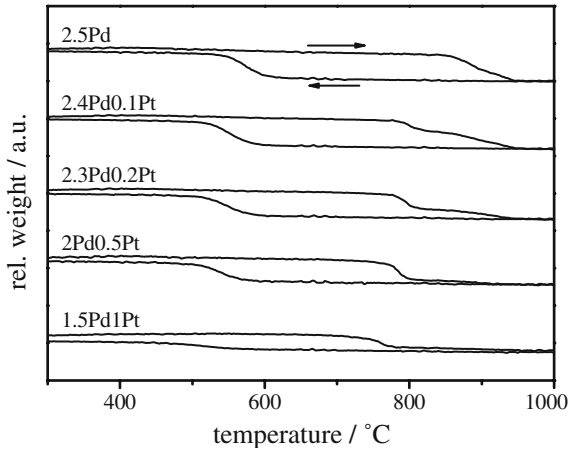

Figure 7. TGA profiles (2nd cycle) of bimetallic Pd–Pt catalysts with different Pt mass fractions. The arrows indicate the profiles during heating and cooling.

Concerning re-oxidation of Pd, Pt addition shifted the re-oxidation point towards lower temperatures, and resulted in flattened re-oxidation profiles. This indicates that platinum kinetically inhibits the re-oxidation of palladium, since the large hysteresis in Pd reduction/re-oxidation is usually attributed to a kinetically inhibited re-oxidation process of palladium [33]. From these results, it can be concluded that platinum addition stabilizes palladium in its reduced form.

3.2. Methane combustion

The as-prepared bimetallic catalysts were tested towards their deactivation during methane combustion by cycling the temperature 4 times between 200 and

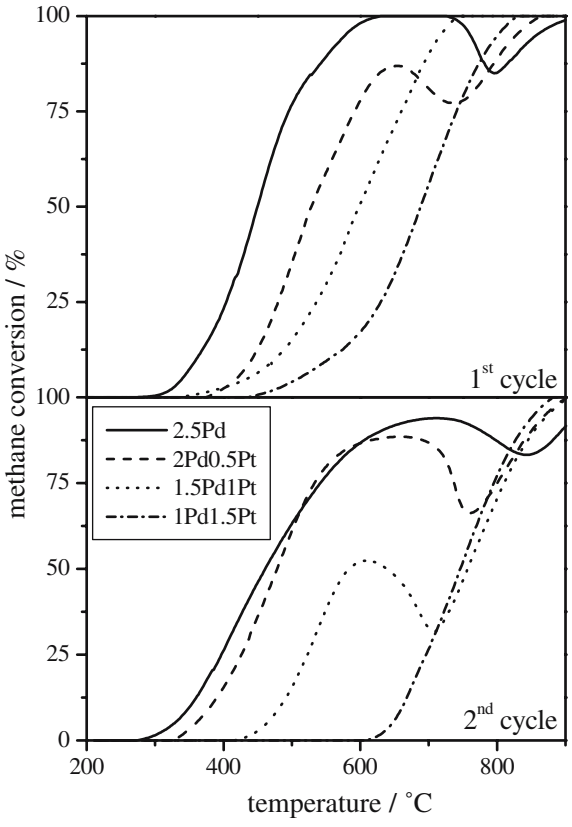

Figure 8. Transient behavior in methane combustion of bimetallic Pd–Pt catalysts during cycles 1 and 2.

1000 °C. Figure 8 depicts the transient behavior in methane combustion of flame-made materials with different Pt mass fractions during cycles 1 and 2. The conditioning attributed to sintering and restructuring of the catalysts during the first cycle, led to significantly different activity profiles for the later cycles. Catalysts with low Pt mass fractions were activated, whereas a high Pt content resulted in a deactivation during the first cycle. In the first cycle, materials with a low Pt mass fraction ($W \leq 20\%$) showed "Pd-like" activity profiles with a distinct decrease in methane conversion between 600 and 800 °C, generally attributed to the reduction of PdO into less active Pd [34]. In contrast, catalysts with a higher Pt mass fraction ($W \geq 40\%$) exhibited "Pt-like" activity profiles without deactivation due to PdO decomposition. Ersson *et al.* [4] found a similar transient behavior for bimetallic Pd–Pt catalysts. The conditioning during the first cycle resulted in a change from a "Pt-like" to a "Pd-like" profile for the catalyst with a Pt weight fraction of 40% (1.5Pd1Pt). Corroborating the results of thermogravimetric analysis in air (figure 7), platinum stabilized palladium in its reduced form and shifted the onset of deactivation (by the PdO → Pd transformation) towards lower temperatures.

Figure 9 depicts the deactivation of bimetallic Pd–Pt catalysts in terms of the temperature needed for 20% methane conversion (T_{20}). After an initial conditioning in a first temperature cycle all catalysts deactivated during the following cycles, indicated by higher temperatures needed for 20% conversion. This deactivation can be attributed to the sintering of the active palladium particles at the high temperatures of up to 1000 °C. The addition of platinum slowed down this deactivation process resulting in lower temperatures needed to achieve the same conversion. Different authors observed similar stabilization effects for Pd combustion catalysts made by impregnation techniques and reported a maximum in activity and stability for Pt mass fractions in the range of 20–40% [4,5,7,35]. Here however, a lower platinum mass fraction of 4% turned out to be an optimal compromise between slower deactivation and lower intrinsic activity, due to the lower activity of Pt compared to Pd, and resulted in the highest activity after several cycles. This stabilization is mainly caused by the beneficial effect of platinum on the sintering behavior of the palladium particles containing small amounts of platinum. This is further confirmed by the CO-chemisorption measurements of annealed catalysts (figure 4).

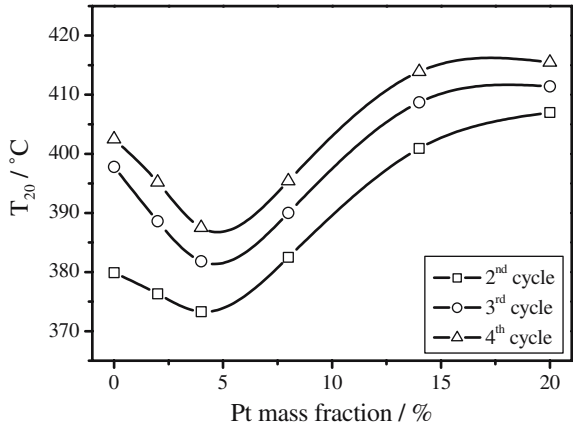

Figure 9. Deactivation of catalysts with different Pd–Pt ratios as expressed by the temperature of 20% methane conversion (T_{20}) during cycles 2–4 (200–1000 °C).

4. Conclusions

Flame-spray pyrolysis has been applied for the one-step synthesis of alumina-supported bimetallic Pd–Pt catalysts. These catalysts were tested in the combustion of methane in the temperature range up to 1000 °C. The as-prepared materials consisted of agglomerated alumina nanoparticles on which the metal components are well-dispersed. After reduction the metal constituents formed small bimetallic particles supported on alumina. EDX and EXAFS measurements indicated that the metal particles are alloyed. Platinum influenced the PdO ↔ Pd transformation, favoring palladium in its reduced form. Furthermore, added in small amounts (Pt mass fraction <10%), platinum increased the resistance of the metal particles towards sintering at high temperatures. This stabilization by Pt improved the behavior of the catalysts in the combustion of methane.

Acknowledgments

We thank Dr. Frank Krumeich (ETH) for the STEM and EDXS measurements, the Hamburger Synchrotron-Strahlungslabor (HASYLAB at DESY) for providing beamtime at beamline X1 and M. Hermann, and J. Wienold for their kind help during our measurements. Financial support by the Swiss Commission for Technology and Innovation (KTI) and the Swiss Federal Institute of Technology (ETH) is kindly acknowledged.

References

[1] G. Centi, J. Mol. Catal. A-Chem. 173 (2001) 287.
[2] D. Ciuparu, M.R. Lyubovsky, E. Altman, L.D. Pfefferle and A. Datye, Catal. Rev.-Sci. Eng. 44 (2002) 593.
[3] P. Gélin and M. Primet, Appl. Catal. B-Environ. 39 (2002) 1.
[4] A. Ersson, H. Kušar, R. Carroni, T. Griffin and S. Järås, Catal. Today 83 (2003) 265.
[5] K. Narui, H. Yata, K. Furuta, A. Nishida, Y. Kohtoku and T. Matsuzaki, Appl. Catal. A-Gen. 179 (1999) 165.
[6] C. Micheaud, P. Marécot, M. Guérin and J. Barbier, Appl. Catal. A-Gen. 171 (1998) 229.
[7] C.L. Pieck, C.R. Vera, E.M. Peirotti and J.C. Yori, Appl. Catal. A-Gen. 226 (2002) 281.
[8] B. Coq and F. Figueras, J. Mol. Catal. A-Chem. 173 (2001) 117.

[9] J. Barbier, in: *Handbook of Heterogeneous Catalysis*, Vol. 1, (eds.) G. Ertl, H. Knözinger, and J. Weitkamp (Wiley-VCH, Weinheim, 1997) 257.
[10] J.P. Candy, B. Didillon, E.L. Smith, T.B. Shay and J.M. Basset, J. Mol. Catal. 86 (1994) 179.
[11] B.C. Gates, Stud. Surf. Sci. Catal. 29 (1986) 415.
[12] J.H. Sinfelt, *Bimetallic Catalysts* (J. Wiley & Sons Inc., New York, 1983)Exxon Monograph.
[13] N. Toshima, M. Harada, T. Yonezawa, K. Kushihashi and K. Asakura, J. Phys. Chem. 95 (1991) 7448.
[14] S.N. Reifsnyder and H.H. Lamb, J. Phys. Chem. B 103 (1999) 321.
[15] P.L. Hansen, A.M. Molenbroek and A.V. Ruban, J. Phys. Chem. B 101 (1997) 1861.
[16] L.E. Aleandri, H. Bönnemann, D.J. Jones, J. Richter and J. Rozière, J. Mater. Chem. 5 (1995) 749.
[17] T. Johannessen, J.R. Jenson, M. Mosleh, J. Johansen, U. Quaade and H. Livbjerg, Chem. Eng. Res. Des. 82 (2004) 1444.
[18] T. Johannessen and S. Koutsopoulos, J. Catal. 205 (2002) 404.
[19] R. Strobel, W.J. Stark, L. Mädler, S.E. Pratsinis and A. Baiker, J. Catal. 213 (2003) 296.
[20] R. Strobel, F. Krumeich, W.J. Stark, S.E. Pratsinis and A. Baiker, J. Catal. 222 (2004) 307.
[21] L. Mädler, W.J. Stark and S.E. Pratsinis, J. Mater. Res. 18 (2003) 115.
[22] S.E. Pratsinis, Prog. Energy Combust. Sci. 24 (1998) 197.
[23] R. Strobel, S.E. Pratsinis and A. Baiker, J. Mater. Chem. 15 (2005) 605.
[24] L. Mädler, H.K. Kammler, R. Mueller and S.E. Pratsinis, J. Aerosol. Sci. 33 (2002) 369.
[25] J.D. Grunwaldt, M. Caravati, S. Hannemann and A. Baiker, Phys. Chem. Chem. Phys. 6 (2004) 3037.
[26] B.S. Clausen, G. Steffensen, B. Fabius, J. Villadsen, R. Feidenhansl and H. Topsøe, J. Catal. 132 (1991) 524.
[27] T. Ressler, J. Synchr. Radiat. 5 (1998) 118.
[28] S.I. Zabinsky, J.J. Rehr, A. Ankudinov, R.C. Albers and M.J. Eller, Phys. Rev. B 52 (1995) 2995.
[29] J.D. Grunwaldt, M. Maciejewski and A. Baiker, Phys. Chem. Chem. Phys. 5 (2003) 1481.
[30] D. Bazin, A. Triconnet and P. Moureaux, Nucl. Instrum. Method Phys. Res. B 97 (1995) 41.
[31] N. Matsubayashi, H. Yasuda, M. Imamura and Y. Yoshimura, Catal. Today 45 (1998) 375.
[32] M. Boudart and H.S. Hwang, J. Catal. 39 (1975) 44.
[33] R.J. Farrauto, M.C. Hobson, T. Kennelly and E.M. Waterman, Appl. Catal. A-Gen. 81 (1992) 227.
[34] A.K. Datye, J. Bravo, T.R. Nelson, P. Atanasova, M. Lyubovsky and L. Pfefferle, Appl. Catal. A-Gen. 198 (2000) 179.
[35] M. Skoglundh, L.O. Löwendahl and J.E. Ottersted, Appl. Catal. 77 (1991) 9.